Geophysical Research Letters

RESEARCH LETTER
10.1029/2020GL091265

Special Section:
The COVID-19 pandemic: linking health, society and environment

Global Significant Changes in Formaldehyde (HCHO) Columns Observed From Space at the Early Stage of the COVID-19 Pandemic

Wenfu Sun[1], Lei Zhu[1], Isabelle De Smedt[2], Bin Bai[1], Dongchuan Pu[1], Yuyang Chen[1], Lei Shu[1], Dakang Wang[1], Tzung-May Fu[1], Xiaofei Wang[3], and Xin Yang[1]

[1]School of Environmental Science and Engineering, Southern University of Science and Technology, Shenzhen, China, [2]Division of Atmospheric Composition, Royal Belgian Institute for Space Aeronomy (BIRA-IASB), Brussels, Belgium, [3]Department of Environmental Science and Engineering, Shanghai Key Laboratory of Atmospheric Particle Pollution and Prevention, Fudan University, Shanghai, China

Key Points:

- We detect significant changes in HCHO columns worldwide at the early stage of the COVID-19 pandemic
- We see evidence of changing atmospheric oxidizing capacity and NMVOC emissions in the Northern China Plain due to the massive lockdown
- Besides anthropogenic emission, temperature and open fires are vital factors dominating variations in HCHO columns

Supporting Information:

- Supporting Information S1

Correspondence to:
L. Zhu,
zhul3@sustech.edu.cn

Citation:
Sun, W., Zhu, L., De Smedt, I., Bai, B., Pu, D., Chen, Y., et al. (2021). Global significant changes in formaldehyde (HCHO) columns observed from space at the early stage of the COVID-19 pandemic. *Geophysical Research Letters*, *48*, e2020GL091265. https://doi.org/10.1029/2020GL091265

Received 13 OCT 2020
Accepted 8 JAN 2021

Abstract Satellite HCHO data are widely used as a reliable proxy of non-methane volatile organic compounds (NMVOCs) to constrain underlying emissions and chemistry. Here, we examine global significant changes in HCHO columns at the early stage of the COVID-19 pandemic (January–April 2020) compared with the same period in 2019 with observations from the TROPOspheric Monitoring Instrument (TROPOMI). HCHO columns decline (11.0%) in the Northern China Plain (NCP) because of a combination of meteorological impacts, lower HCHO yields as NO_x emission plunges (by 36.0%), and reduced NMVOC emissions (by 15.0%) resulting from the lockdown. HCHO columns change near Beijing (+8.4%) due mainly to elevated hydroxyl radical as NO_x emission decreases in a NO_x-saturated regime. HCHO columns change in Australia (+17.5%), Northeastern Myanmar of Southeast Asia (+14.9%), Central Africa (+7.8%), and Central America (+18.9%), consistent with fire activities. Our work also points to other changes related to temperature and meteorological variations.

Plain Language Summary We use satellite observations to examine global significant changes in HCHO columns at the early stage of the COVID-19 pandemic compared with the same period in 2019. HCHO columns decreased in the Northern China Plain caused by a joint effect of meteorology, reduced anthropogenic NO_x, and decreased non-methane volatile organic compound emissions during the lockdown. The impact of temperature and meteorology on HCHO columns is observed in Northwestern China, India, Southern Africa, Eastern Brazil, Southern Cone, and Northeastern Thailand of Southeast Asia. Regional changes in Southeastern Australia, Northeastern Myanmar of Southeast Asia, Central Africa, and Central America are likely driven by open fire activities.

1. Introduction

The COVID-19 pandemic outbreak has reshaped normal social and economic activities dramatically, resulting in sudden changes in the emissions of air pollutants and their precursors. Recent air quality-related studies predominantly focus on the impacts of plunged nitrogen oxides (NO_x) emission (Bauwens et al., 2020; Liu et al., 2020; Menut et al., 2020; Venter et al., 2020; Zangari et al., 2020; R. Zhang et al., 2020) on particulate matters (Chang et al., 2020; G. He et al., 2020; Kumar et al., 2020; Shi & Brasseur, 2020; Venter et al., 2020; Zangari et al., 2020) and surface ozone (G. He et al., 2020; Le et al., 2020; Shi & Brasseur, 2020; Siciliano et al., 2020; Venter et al., 2020). Here, we use formaldehyde (HCHO) columns from the TROPOspheric Monitoring Instrument (TROPOMI) (Veefkind et al., 2012) to examine global changes in HCHO at the early stage of the COVID-19 pandemic (hereafter defined as January–April 2020) and relate them to variations in anthropogenic emissions of non-methane volatile organic compounds (NMVOCs), temperature, and open fires.

HCHO is detectable from space as a vertical column density (VCD) using solar ultraviolet backscattered radiation between 325 and 360 nm (Chance et al., 2000). Owing to its short atmospheric lifetime (a few hours against oxidation and photolysis) and high production yields from the oxidation of NMVOCs, HCHO VCD has been applied as a localized proxy for NMVOC emissions from biogenic sources (Palmer et al., 2003;

Shim et al., 2005; Surl et al., 2018; Y. Zhang et al., 2019), anthropogenic sources (Fu et al., 2007; Shen et al., 2019; L. Zhu et al., 2014), and open fires (Gonzi et al., 2011; Shim et al., 2005; Y. Zhang et al., 2019).

In this study, we use HCHO data available from the recently launched TROPOMI to examine how HCHO changes from January–April 2019 to January–April 2020, building on our oversampling method (Sun et al., 2018; L. Zhu et al., 2014; L. Zhu, Jacob, et al., 2017), and identifying significance through allocating satellite pixels by their corresponding temperatures (L. Zhu, Mickley, et al., 2017)

2. Significant Changes in TROPOMI HCHO Columns

TROPOMI is a nadir-viewing hyperspectral spectrometer onboard the Copernicus Sentinel-5 Precursor platform launched in October 2017. It scans the whole globe daily at a local time of 13:30. We use the TROPOMI HCHO product (De Smedt et al., 2018) based on the technical heritage of retrieving HCHO from the Global Ozone Monitoring Experiment (GOME), GOME-2, and Ozone Monitoring Instrument (OMI) (De Smedt et al., 2018). TROPOMI HCHO product offers the finest nadir spatial resolution (7 km × 3.5 km, upgraded to 5.5 km × 3.5 km since August 2019) with a high signal-to-noise ratio among currently available HCHO products. The product correlates highly with Multi-AXis Differential Optical Absorption Spectroscopy ($r = 0.88$) and Fourier-transform infrared ($r = 0.91$) measurements with a mean bias ranging from −26.0% to +30.8%, depending on locations (Chan et al., 2020; Vigouroux et al., 2020).

We select TROPOMI level-2 pixels with (1) quality assurance value greater than 0.5, (2) cloud fraction less than 0.3, and (3) solar zenith angle less than 60°. This study focuses on examining significant mean changes in HCHO columns from January–April 2019 to January–April 2020, rather than investigating daily or weekly variations. We follow L. Zhu, Mickley, et al. (2017) to group TROPOMI pixels by their associated temperatures to identify significant changes between the two periods. Unlike focusing on a long-term HCHO trend in L. Zhu, Mickley, et al. (2017), those changes between two sets of 4-month observations are still influenced by monotonous temperature changes.

Briefly, we first assign a temperature value to each level-2 pixel based on its location and observing time, using hourly surface air temperature data (0.5° × 0.625°) from the Modern-Era Retrospective Analysis for Research and Applications, version 2 (MERRA-2) (Gelaro et al., 2017). We then allocate all pixels into 200 temperature bins ranging from 273 to 323 K with an increment of 0.25 K. For each bin i, we use our oversampling method (Sun et al., 2018; L. Zhu et al., 2014; L. Zhu, Jacob, et al., 2017) to map mean January–April HCHO columns in 2019 and 2020 onto 0.5° × 0.5° grids (j), denoted as $\bar{\Omega}_{i,j,2019}$ and $\bar{\Omega}_{i,j,2020}$, respectively. We determine this spatial resolution based on a satellite detection capability and overlapping pixels amount over a grid cell. The change in HCHO columns in temperature i for grid cell j is written as

$$\Delta\bar{\Omega}_{i,j} = \bar{\Omega}_{i,j,2020} - \bar{\Omega}_{i,j,2019} \tag{1}$$

We further compute the change for each grid cell j ($\Delta\bar{\Omega}_j$) as the mean of changes across all bins with at least 30 overlapping pixels, weighted by the total number of overlapping pixels in each bin:

$$\Delta\bar{\Omega}_j = \frac{\sum_i \Delta\bar{\Omega}_{i,j}\left(N_{i,j,2019} + N_{i,j,2020}\right)}{\sum_i N_{i,j,2019} + N_{i,j,2020}} \tag{2}$$

where $N_{i,j,2019}$ and $N_{i,j,2020}$ represent the number of overlapping pixels for grid cell j in temperature bin i for January–April of 2019 and 2020. We consider only grid cells with values from at least 50 temperature bins so that each $\Delta\bar{\Omega}_j$ is contributed by more than 1,500 pixels. We restrict our following analysis to grid cells with significant nonzero $\Delta\bar{\Omega}_j$, determined with the t test (p-value < 0.05). Here and elsewhere, changes in TROPOMI HCHO columns are significant, unless otherwise stated. We also try a finer spatial resolution of 0.05° × 0.05° and 0.25° × 0.25° but find that it becomes difficult to obtain statistically significant outcomes from smaller sample sizes.

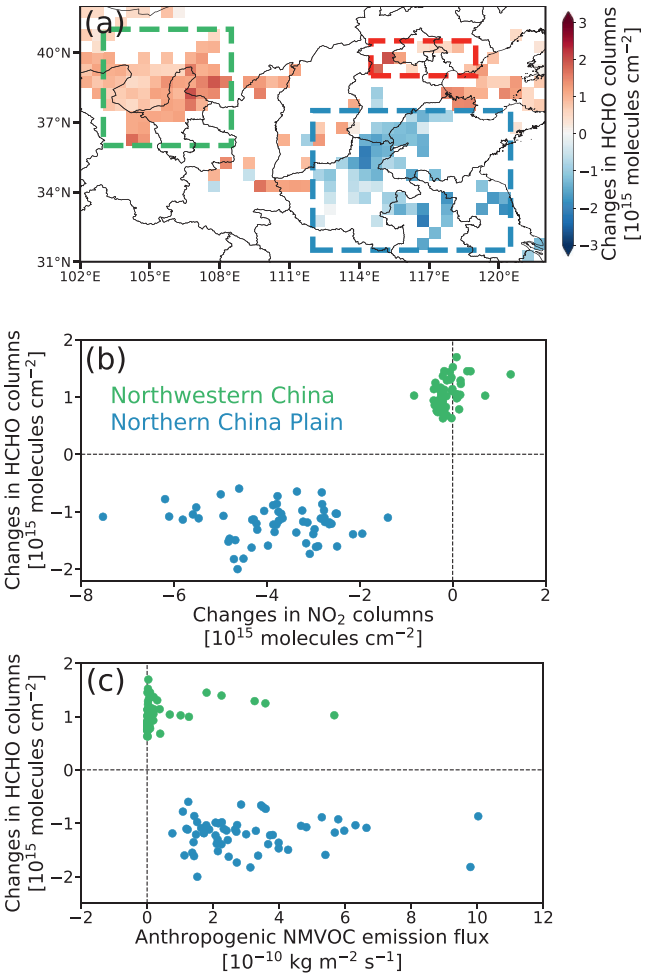

Figure 1. Significant changes in mean TROPOMI HCHO columns at the early stage of the pandemic (defined as January–April 2020) in (a) Northern China and its respective relations to (b) changes in TROPOMI NO_2 columns and (c) anthropogenic NMVOC emissions. Changes are computed as the difference in mean columns from January–April 2019 to January–April 2020. The blue and green dots in (b) and (c) represent individual 0.5° × 0.5° grid cells with HCHO changes in the Northern China Plain (NCP; the blue box in (a); 112°E–120.5°E, 31.5°N–37.5°N) and Northwestern China (the green box in (a); 103°E–108.5°E, 36°N–41°N), respectively. The red box (114.5°E–119°E, 39°N–40.5°N) contains several grid cells near Beijing. TROPOMI NO_2 pixels (van Geffen et al., 2020) are selected using the same criteria as HCHO pixels (see text) and are oversampled (without being grouped by temperatures) onto the 0.5° × 0.5° grids for the respective two periods. Anthropogenic NMVOC emissions are from the mosaic Asian anthropogenic emission inventories (MIX) (Li et al., 2017). TROPOMI, TROPOspheric Monitoring Instrument; NMVOC, non-methane volatile organic compound.

3. Results and Discussions

As shown in Figure 1(a), HCHO columns decline on average by 11.0% ± 2.8% in the Northern China Plain (NCP) at the early stage of the COVID-19 pandemic compared with the same period in 2019. Such a decrease is not driven by temperature (+0.7 K; Table S1) and not fully due to meteorological variations which only result in a 5.7% decrease in HCHO columns (Table S1). HCHO reductions are generally located at grid cells with predominant declines in NO_2 columns (Figure 1(b)) and relatively high anthropogenic NMVOC emissions (Figure 1(c)), suggesting a linkage between reductions in HCHO columns and perturbations of anthropogenic emissions resulting from the massive lockdown. However, such a linkage is likely complicated by (1) varying HCHO production yields resulted from different NO_x levels (Wolfe et al., 2016; L. Zhu, Mickley, et al., 2017) as Chinese NO_x emission plunges in this period (Bauwens et al., 2020; Feng et al., 2020; Liu et al., 2020; Miyazaki et al., 2020; Shi & Brasseur, 2020) and (2) changing anthropogenic NMVOC emissions in the NCP, a region characterized by intense industry activities (Li et al., 2019).

To tease out contributions by the above two factors, we conduct a series of sensitivity simulations with the GEOS-Chem (http://www.geos-chem.org, version 12) 3-D chemical transport model. We scale down NO_x and NMVOC emissions to simultaneously reproduce the mean reduction in NO_2 (42.2%) and HCHO (11.0%) column seen by TROPOMI in the NCP. GEOS-Chem is reliable in modeling the observed relationship between HCHO columns and NMVOC emissions (Fu et al., 2007; Palmer et al., 2003; Shen et al., 2019; Surl et al., 2018; L. Zhu et al., 2016, 2020) under various NO_x conditions (Travis et al., 2016; L. Zhu, Mickley, et al., 2017). Here, we run the GEOS-Chem model (2° × 2.5°) from January 2018 to April 2020, driven by the MERRA-2 meteorological fields (Gelaro et al., 2017). The model uses biogenic VOC emissions from the MEGAN v2.1 (Guenther et al., 2012), open fire emissions from the fourth-generation global fire emissions database (Giglio et al., 2013), and anthropogenic emissions from the MIX inventory (Li et al., 2017) over Asia. We sample GEOS-Chem outputs according to the TROPOMI schedule and then grid the model results to the same 0.5° × 0.5° grids of satellite observations. We acknowledge the coarse model resolution, which may not lead to biases as small-scale nonlinearities may have an insignificant impact on regional analysis (Yu et al., 2016).

Figure 2 summarizes how modeled mean NO_2 and HCHO columns in the NCP respond to the scaling-down of NO_x and NMVOC emissions. NO_2 column reduction correlates almost linearly with the decrease in NO_x emissions on the regional scale. GEOS-Chem reproduces the observed reduction in mean NO_2 column (42.2%) in the NCP when applying a uniform decrease of 36.0% in anthropogenic NO_x emissions. The result takes the difference in meteorological conditions between 2019 and 2020 into consideration by running the GEOS-Chem model with corresponding meteorological fields. Our finding is consistent with the recently estimated reductions in NO_2 (40%–60%) and NO_x (36%–48%) in China during the COVID-19 pandemic (Bauwens et al., 2020; Feng et al., 2020; Liu et al., 2020; Miyazaki et al., 2020; Shi & Brasseur, 2020).

We see from Figure 2(a) that the declining NO_x emission leads to additional lower HCHO columns in the NCP. This is due to the slower conversion of HO_2 to OH caused by lower NO, which decelerates HCHO production from the oxidation of NMVOCs (Wolfe et al., 2016; L. Zhu, Jacob, et al., 2017; L. Zhu, Mickley, et al., 2017). Reducing NO_x emissions by 36.0% as constrained by TROPOMI NO_2 observations results in

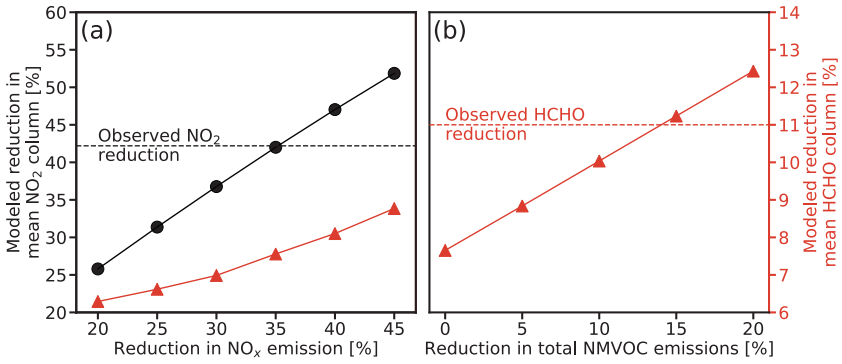

Figure 2. Responses of modeled reductions in mean NO_2 and HCHO columns in the Northern China Plain (NCP) to the scaling-down of NO_x and NMVOC emissions. (a) Reductions in mean NO_2 (black dots) and HCHO columns (red triangles) due to declining NO_x emissions. The black dashed line demonstrates the decrease (42.2%) in mean NO_2 columns from January–April 2019 to January–April 2020 in the NCP, as observed by TROPOMI. (b) Reductions in mean HCHO columns (red triangles) due to declining NMVOC emissions (with a fixed reduction of 36.0% in NO_x emission to match the observed decrease in TROPOMI NO_2 columns). The red dashed line shows the reduction (11.0%) in mean HCHO columns according to TROPOMI. Model results are from a series of GEOS-Chem sensitivity simulations run at 2.0° × 2.5°. NMVOC, non-methane volatile organic compound; TROPOMI, TROPOspheric Monitoring Instrument.

only a 7.7% decline in the mean HCHO column in the NCP, inconsistent with the reduction according to TROPOMI (11.0%; Figure 1). This suggests that anthropogenic NMVOC emissions in the NCP probably also decrease at the early stage of the pandemic. Our simulations (Figure 2(b)) show that introducing an additional 15.0% reduction in anthropogenic NMVOC emissions is necessary to fill the gap, simultaneously reproducing observed mean reduction in both NO_2 and HCHO columns in the NCP. Here, the scaling factors are applied to all emission sectors. We acknowledge that NO_x and NMVOC emissions from some sectors may have changed differently during the lockdown, and detailed atmospheric chemical relationship in urban scale deserves future exploration.

Figure 1(a) also shows that the mean HCHO column increases on average by 8.4% ± 4.2% over a few grid cells near Beijing. We attribute this to a faster HCHO production rate through the oxidation of NMVOCs, driven by higher OH levels as NO_x emission decreases (by 17.0%, according to TROPOMI NO_2 columns) in a NO_x-saturated regime. GEOS-Chem results confirm that the mean surface OH level increases by 14.5% ± 3.3% in this region during this period due both to a reduction in NO_x emissions (8.2%) and changes in meteorological conditions (6.3%).

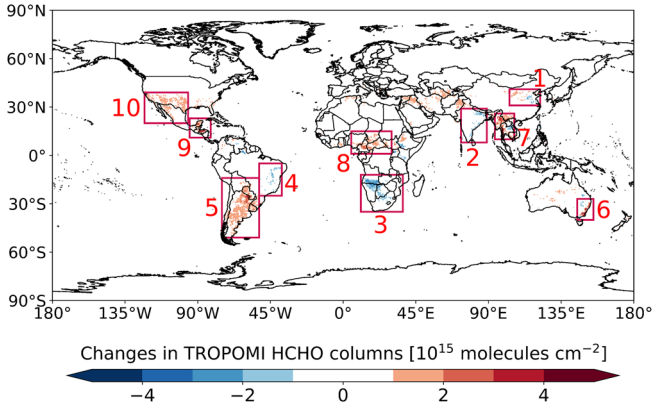

Figure 3. Global significant changes in HCHO columns (0.5° × 0.5°) at the early stage of the pandemic, computed as the difference in mean TROPOMI HCHO columns from January–April 2019 to January–April 2020. Changes in 10 regions are examined in the text and labeled in order 1–10: Northern China (same as the domain shown in Figure 1(a)), India, Southern Africa, Eastern Brazil, Southern Cone, Southeastern Australia, Southeast Asia, Central Africa, Central America, and the Southwestern United States and Northern Mexico. TROPOMI, TROPOspheric Monitoring Instrument.

The mean HCHO column raises by 14.2% ± 3.1% in Northwestern China (Figure 1(a)). This region is characterized by weak reductions in NO_2 columns (Figure 1(b)) and low anthropogenic NMVOC emissions (Figure 1(c)), implying variations in meteorological conditions rather than anthropogenic emissions as the main driver. The surface temperature increases by 1.0 K on average, which translates to an increase of 11.1% in HCHO columns (Table S1), assuming an exponential dependence on temperature (Palmer et al., 2006; L. Zhu et al., 2014). Acknowledging such temperature dependence is from regional/local studies, we attribute HCHO changes here qualitatively to temperature variations. GEOS-Chem fails to reproduce the HCHO increase in this region (Table S1), implying the impact of temperature has likely been over-compensated by other factors in the model when HCHO is low.

In Figure 3, we extend our analysis to examine global changes in HCHO columns at the early stage of the pandemic. In India (Region 2), the mean HCHO column decreases by 7.0% ± 2.9% on a subcontinental scale, consistent with modeled reduction (6.3%) due to meteorological difference (Table S1). HCHO reduction is also roughly consistent with an estimated

reduction (9.8%) when applying the temperature dependence (Table S1). Those findings likely reflect the dominant influence of temperature (−0.9 K) in biogenic isoprene emission, thus on HCHO columns in India (Surl et al., 2018). We observe similar temperature-dominated influence on HCHO columns in Southern Africa (Region 3; −11.7% ± 6.4%), Eastern Brazil (Region 4; −10.1% ± 4.6%), Southern Cone (Region 5; +13.5% ± 5.1%), and Northeastern Thailand in Southeast Asia (Region 7; −11.2% ± 2.5%), where regional mean temperature changes respectively by −1.8, −1.0, +0.8, and −1.4 K, as summarized in Table S1.

The increase in HCHO columns in Southeastern Australia (Region 6; 17.5% ± 10.7%) may be traced to exceptionally high open fire emissions at the beginning of 2020, but not meteorological variations (Table S1). Using the Global Fire Assimilation System (GFAS) data (Kaiser et al., 2012), we find mean non-methane hydrocarbon (NMHC) emission flux increases by a factor of ∼7.0 in this region. We see similar correlations between changes in HCHO columns and fire activities in Northeastern Myanmar in Southeast Asia (Region 7; +14.9% ± 3.4%), Central Africa (Region 8, +7.8% ± 3.7%), and Central America (Region 9; +18.9% ± 7.8%), where regional mean NMHC emission flux changes by +28.4%, +18.5%, and +19.5%. Those regions are known for high fire-driven HCHO columns (Marbach et al., 2008; Stavrakou et al., 2015). However, quantifying the impact of fire emissions on HCHO columns is challenging because of the uncertainties in diurnal variations and emission factors of wildfires. In the Southwestern United States and Northern Mexico (Region 10), the mean HCHO column increases by 12.2% ± 0.1% with unclear reasons (Table S1).

The lack of significant anthropogenic signals outside the NCP at the early stage of the COVID-19 pandemic (Figure 3) is consistent with the lockdown timeline worldwide. We acknowledge that the absence of TROPOMI HCHO observations before May 2018 limits the long-term analysis of HCHO columns. Although OMI HCHO (González Abad et al., 2015) has been widely used for long-term trend analysis (De Smedt et al., 2015; Shen et al., 2019; L. Zhu, Mickley, et al., 2017b; S. Zhu et al., 2018), we find OMI fails to detect significant HCHO changes (Figure S1 and Text S1). This is due to inadequate valid observations from OMI, thus emphasizing the value of TROPOMI data. Future studies to investigate interannual and urban-scale variabilities in HCHO columns and NMVOC emissions may become available as a longer span of TROPOMI HCHO product or Geostationary HCHO observations (Kim et al., 2020; Kwon et al., 2019) are ready.

4. Conclusion

We have used TROPOMI satellite observations to examine significant changes in HCHO columns at the early stage of the COVID-19 pandemic over the globe. We find regional decline driven by reduced anthropogenic nitrogen oxides (NO_x) and NMVOC emissions in the NCP. Regional changes in Northwestern China, India, Southern Africa, Eastern Brazil, Southern Cone, and Northeastern Thailand may be traced to variations in temperatures. The impact of open fires on HCHO columns is also identified in Southeastern Australia, Northeastern Myanmar, Central Africa, and Central America. Our study highlights the importance of TROPOMI satellite observations in understanding variations in anthropogenic emissions by providing evidence from space.

Data Availability Statement

The GEOS-Chem 3-D Chemical Transport Model is available at http://www.geos-chem.org.

Acknowledgments
This work is supported by the Center for Computational Science and Engineering at Southern University of Science and Technology and Guangdong University Youth Innovation Talent Project (2020KQNCX066). We gratefully acknowledge the data set of TROPOMI HCHO and NO_2 product (https://disc.gsfc.nasa.gov/), MERRA-2 (https://gmao.gsfc.nasa.gov/reanalysis/MERRA-2/), MIX inventory (http://meicmodel.org/?lang = en), and GFAS (https://www.ecmwf.int/en/forecasts/dataset/global-fire-assimilation-system).

References

Bauwens, M., Compernolle, S., Stavrakou, T., Müller, J. F., Gent, J., Eskes, H., et al. (2020). Impact of coronavirus outbreak on NO_2 pollution assessed using TROPOMI and OMI observations. *Geophysical Research Letters*, *47*, e2020GL087978. https://doi.org/10.1029/2020GL087978

Chan, K. L., Wiegner, M., van Geffen, J., De Smedt, I., Alberti, C., Cheng, Z., et al. (2020). MAX-DOAS measurements of tropospheric NO_2 and HCHO in Munich and the comparison to OMI and TROPOMI satellite observations. *Atmospheric Measurement Techniques*, *13*(8), 4499–4520. https://doi.org/10.5194/amt-13-4499-2020

Chance, K., Palmer, P. I., Spurr, R. J. D., Martin, R. V., Kurosu, T. P., & Jacob, D. J. (2000). Satellite observations of formaldehyde over North America from GOME. *Geophysical Research Letters*, *27*(21), 3461–3464. https://doi.org/10.1029/2000GL011857

Chang, Y., Huang, R. J., Ge, X., Huang, X., Hu, J., Duan, Y., et al. (2020). Puzzling haze events in China during the coronavirus (COVID-19) shutdown. *Geophysical Research Letters*, *47*, e2020GL088533. https://doi.org/10.1029/2020GL088533

De Smedt, I., Stavrakou, T., Hendrick, F., Danckaert, T., Vlemmix, T., Pinardi, G., et al. (2015). Diurnal, seasonal and long-term variations of global formaldehyde columns inferred from combined OMI and GOME-2 observations. *Atmospheric Chemistry and Physics*, *15*(21), 12519–12545. https://doi.org/10.5194/acp-15-12519-2015

De Smedt, I., Theys, N., Yu, H., Danckaert, T., Lerot, C., Compernolle, S., et al. (2018). Algorithm theoretical baseline for formaldehyde retrievals from S5P TROPOMI and from the QA4ECV project. *Atmospheric Measurement Techniques*, *11*(4), 2395–2426. https://doi.org/10.5194/amt-11-2395-2018

Feng, S., Jiang, F., Wang, H., Wang, H., Ju, W., Shen, Y., et al. (2020). NO_x emission changes over China during the COVID-19 epidemic inferred from surface NO_2 observations. *Geophysical Research Letters*, *47*, e2020GL090080. https://doi.org/10.1029/2020GL090080

Fu, T.-M., Jacob, D. J., Palmer, P. I., Chance, K., Wang, Y. X., Barletta, B., et al. (2007). Space-based formaldehyde measurements as constraints on volatile organic compound emissions in east and south Asia and implications for ozone. *Journal of Geophysical Research*, *112*, D06312. https://doi.org/10.1029/2006JD007853

Gelaro, R., McCarty, W., Suarez, M. J., Todling, R., Molod, A., Takacs, L., et al. (2017). The Modern-Era Retrospective Analysis for Research and Applications, Version 2 (MERRA-2). *Journal of Climate*, *30*(14), 5419–5454. https://doi.org/10.1175/JCLI-D-16-0758.1

Giglio, L., Randerson, J. T., & van der Werf, G. R. (2013). Analysis of daily, monthly, and annual burned area using the fourth-generation global fire emissions database (GFED4). *Journal of Geophysical Research: Biogeosciences*, *118*, 317–328. https://doi.org/10.1002/jgrg.20042

González Abad, G., Liu, X., Chance, K., Wang, H., Kurosu, T. P., & Suleiman, R. (2015). Updated Smithsonian Astrophysical Observatory Ozone Monitoring Instrument (SAO OMI) formaldehyde retrieval. *Atmospheric Measurement Techniques*, *8*(1), 19–32. https://doi.org/10.5194/amt-8-19-2015

Gonzi, S., Palmer, P. I., Barkley, M. P., De Smedt, I., & Van Roozendael, M. (2011). Biomass burning emission estimates inferred from satellite column measurements of HCHO: Sensitivity to co-emitted aerosol and injection height. *Geophysical Research Letters*, *38*, L14807. https://doi.org/10.1029/2011GL047890

Guenther, A. B., Jiang, X., Heald, C. L., Sakulyanontvittaya, T., Duhl, T., Emmons, L. K., & Wang, X. (2012). The Model of Emissions of Gases and Aerosols from Nature version 2.1 (MEGAN2.1): An extended and updated framework for modeling biogenic emissions. *Geoscientific Model Development*, *5*(6), 1471–1492. https://doi.org/10.5194/gmd-5-1471-2012

He, G., Pan, Y., & Tanaka, T. (2020). The short-term impacts of COVID-19 lockdown on urban air pollution in China. *Nature Sustainability*, *3*, 1005–1011. https://doi.org/10.1038/s41893-020-0581-y

He, H., Ren, X., Benish, S. E., Li, Z., Wang, F., Wang, Y., et al (2019). Evaluation of anthropogenic emissions and ozone pollution in the North China Plain: Insights from the Air Chemistry Research in Asia (ARIAs) campaign. *Atmospheric Chemistry and Physics*. https://doi.org/10.5194/acp-2019-248

Kaiser, J. W., Heil, A., Andreae, M. O., Benedetti, A., Chubarova, N., Jones, L., et al. (2012). Biomass burning emissions estimated with a Global Fire Assimilation System based on observed fire radiative power. *Biogeosciences*, *9*(1), 527–554. https://doi.org/10.5194/bg-9-527-2012

Kim, J., Jeong, U., Ahn, M.-H., Kim, J. H., Park, R. J., Lee, H., et al. (2020). New era of air quality monitoring from space: Geostationary Environment Monitoring Spectrometer (GEMS). *Bulletin of the American Meteorological Society*, *101*(1), E1–E22. https://doi.org/10.1175/BAMS-D-18-0013.1

Kumar, P., Hama, S., Omidvarborna, H., Sharma, A., Sahani, J., Abhijith, K. V., et al. (2020). Temporary reduction in fine particulate matter due to 'anthropogenic emissions switch-off' during COVID-19 lockdown in Indian cities. *Sustainable Cities and Society*, *62*, 102382. https://doi.org/10.1016/j.scs.2020.102382

Kwon, H.-A., Park, R. J., Abad, G. G., Chance, K., Kurosu, T. P., Kim, J., et al. (2019). Description of a formaldehyde retrieval algorithm for the Geostationary Environment Monitoring Spectrometer (GEMS). *Atmospheric Measurement Techniques*, *12*(7), 3551–3571. https://doi.org/10.5194/amt-12-3551-2019

Le, T., Wang, Y., Liu, L., Yang, J., Yung, Y. L., Li, G., & Seinfeld, J. H. (2020). Unexpected air pollution with marked emission reductions during the COVID-19 outbreak in China. *Science*, *369*(6504), 702–706. https://doi.org/10.1126/science.abb7431

Li, M., Zhang, Q., Kurokawa, J.-I., Woo, J.-H., He, K., Lu, Z., et al. (2017). MIX: A mosaic Asian anthropogenic emission inventory under the international collaboration framework of the MICS-Asia and HTAP. *Atmospheric Chemistry and Physics*, *17*(2), 935–963. https://doi.org/10.5194/acp-17-935-2017

Li, M., Zhang, Q., Zheng, B., Tong, D., Lei, Y., Liu, F., et al. (2019). Persistent growth of anthropogenic non-methane volatile organic compound (NMVOC) emissions in China during 1990–2017: Drivers, speciation and ozone formation potential. *Atmospheric Chemistry and Physics*, *19*(13), 8897–8913. https://doi.org/10.5194/acp-19-8897-2019

Liu, F., Page, A., Strode, S. A., Yoshida, Y., Choi, S., Zheng, B., et al. (2020). Abrupt decline in tropospheric nitrogen dioxide over China after the outbreak of COVID-19. *Science Advances*, *6*(28), eabc2992. https://doi.org/10.1126/sciadv.abc2992

Marbach, T., Beirle, S., Liu, C., Platt, U., & Wagner, T. (2008). Biomass burning emissions from satellite observations: Synergistic use of formaldehyde (HCHO), fire counts and surface temperature. *Paper presented at the Conference on Remote Sensing of Fire—Science and Application, San Diego, CA*.

Menut, L., Bessagnet, B., Siour, G., Mailler, S., Pennel, R., & Cholakian, A. (2020). Impact of lockdown measures to combat Covid-19 on air quality over western Europe. *The Science of the Total Environment*, *741*, 140426. https://doi.org/10.1016/j.scitotenv.2020.140426

Miyazaki, K., Bowman, K., Sekiya, T., Jiang, Z., Chen, X., Eskes, H., et al. (2020). Air quality response in China linked to the 2019 novel coronavirus (COVID-19) lockdown. *Geophysical Research Letters*, *47*, e2020GL089252. https://doi.org/10.1029/2020GL089252

Palmer, P. I., Abbot, D. S., Fu, T.-M., Jacob, D. J., Chance, K., Kurosu, T. P., et al. (2006). Quantifying the seasonal and interannual variability of North American isoprene emissions using satellite observations of the formaldehyde column. *Journal of Geophysical Research*, *111*, D12315. https://doi.org/10.1029/2005JD006689

Palmer, P. I., Jacob, D. J., Fiore, A. M., Martin, R. V., Chance, K., & Kurosu, T. P. (2003). Mapping isoprene emissions over North America using formaldehyde column observations from space. *Journal of Geophysical Research-Atmospheres*, *108*(D6), 4180. https://doi.org/10.1029/2002JD002153

Shen, L., Jacob, D. J., Zhu, L., Zhang, Q., Zheng, B., Sulprizio, M. P., et al. (2019). The 2005–2016 trends of formaldehyde columns over China observed by satellites: Increasing anthropogenic emissions of volatile organic compounds and decreasing agricultural fire emissions. *Geophysical Research Letters*, *46*, 4468–4475. https://doi.org/10.1029/2019GL082172

Shi, X., & Brasseur, G. P. (2020). The response in air quality to the reduction of Chinese economic activities during the COVID-19 outbreak. *Geophysical Research Letters*, *47*, e2020GL088070. https://doi.org/10.1029/2020GL088070

Shim, C., Wang, Y. H., Choi, Y., Palmer, P. I., Abbot, D. S., & Chance, K. (2005). Constraining global isoprene emissions with Global Ozone Monitoring Experiment (GOME) formaldehyde column measurements. *Journal of Geophysical Research*, *110*, D24301. https://doi.org/10.1029/2004JD005629

Siciliano, B., Dantas, G., da Silva, C. M., & Arbilla, G. (2020). Increased ozone levels during the COVID-19 lockdown: Analysis for the city of Rio de Janeiro, Brazil. *Science of the Total Environment*, *737*, 139765. https://doi.org/10.1016/j.scitotenv.2020.139765

Stavrakou, T., Muller, J. F., Bauwens, M., De Smedt, I., Van Roozendael, M., De Maziere, M., et al. (2015). How consistent are top-down hydrocarbon emissions based on formaldehyde observations from GOME-2 and OMI? *Atmospheric Chemistry and Physics*, *15*(20), 11861–11884. https://doi.org/10.5194/acp-15-11861-2015

Sun, K., Zhu, L., Cady-Pereira, K., Miller, C. C., Chance, K., Clarisse, L., et al. (2018). A physics-based approach to oversample multi-satellite, multispecies observations to a common grid. *Atmospheric Measurement Techniques*, *11*(12), 6679–6701. https://doi.org/10.5194/amt-11-6679-2018

Surl, L., Palmer, P. I., & Abad, G. G. (2018). Which processes drive observed variations of HCHO columns over India? *Atmospheric Chemistry and Physics*, *18*(7), 4549–4566. https://doi.org/10.5194/acp-18-4549-2018

Travis, K. R., Jacob, D. J., Fisher, J. A., Kim, P. S., Marais, E. A., Zhu, L., et al. (2016). Why do models overestimate surface ozone in the Southeast United States? *Atmospheric Chemistry and Physics*, *16*(21), 13561–13577. https://doi.org/10.5194/acp-16-13561-2016

van Geffen, J., Boersma, K. F., Eskesl, H., Sneep, M., ter Linden, M., Zara, M., & Veefkind, J. P. (2020). S5P TROPOMI NO_2 slant column retrieval: Method, stability, uncertainties and comparisons with OMI. *Atmospheric Measurement Techniques*, *13*(3), 1315–1335. https://doi.org/10.5194/amt-13-1315-2020

Veefkind, J. P., Aben, I., McMullan, K., Forster, H., de Vries, J., Otter, G., et al. (2012). TROPOMI on the ESA Sentinel-5 Precursor: A GMES mission for global observations of the atmospheric composition for climate, air quality and ozone layer applications. *Remote Sensing of Environment*, *120*, 70–83. https://doi.org/10.1016/j.rse.2011.09.027

Venter, Z. S., Aunan, K., Chowdhury, S., & Lelieveld, J. (2020). COVID-19 lockdowns cause global air pollution declines. *Proceedings of the National Academy of Sciences of the United States of America*, *117*(32), 18984–18990. https://doi.org/10.1073/pnas.2006853117

Vigouroux, C., Langerock, B., Bauer Aquino, C. A., Blumenstock, T., Cheng, Z., De Maziere, M., et al. (2020). TROPOMI-Sentinel-5 Precursor formaldehyde validation using an extensive network of ground-based Fourier-transform infrared stations. *Atmospheric Measurement Techniques*, *13*(7), 3751–3767. https://doi.org/10.5194/amt-13-3751-2020

Wolfe, G. M., Kaiser, J., Hanisco, T. F., Keutsch, F. N., de Gouw, J. A., Gilman, J. B., et al. (2016). Formaldehyde production from isoprene oxidation across NO_x regimes. *Atmospheric Chemistry and Physics*, *16*(4), 2597–2610. https://doi.org/10.5194/acp-16-2597-2016

Yu, K., Jacob, D. J., Fisher, J. A., Kim, P. S., Marais, E. A., Miller, C. C., et al. (2016). Sensitivity to grid resolution in the ability of a chemical transport model to simulate observed oxidant chemistry under high-isoprene conditions. *Atmospheric Chemistry and Physics*, *16*(7), 4369–4378. https://doi.org/10.5194/acp-16-4369-2016

Zangari, S., Hill, D. T., Charette, A. T., & Mirowsky, J. E. (2020). Air quality changes in New York City during the COVID-19 pandemic. *The Science of the Total Environment*, *742*, 140496. https://doi.org/10.1016/j.scitotenv.2020.140496

Zhang, R., Zhang, Y., Lin, H., Feng, X., Fu, T.-M., & Wang, Y. (2020). NO_x emission reduction and recovery during COVID-19 in east China. *Atmosphere*, *11*(4), 433. https://doi.org/10.3390/atmos11040433

Zhang, Y., Li, R., Min, Q., Bo, H., Fu, Y., Wang, Y., & Gao, Z. (2019). The controlling factors of atmospheric formaldehyde (HCHO) in Amazon as seen from satellite. *Earth and Space Science*, *6*, 959–971. https://doi.org/10.1029/2019EA000627

Zhu, L., González Abad, G., Nowlan, C. R., Chan Miller, C., Chance, K., Apel, E. C., et al. (2020). Validation of satellite formaldehyde (HCHO) retrievals using observations from 12 aircraft campaigns. *Atmospheric Chemistry and Physics*, *20*, 12329–12345. https://doi.org/10.5194/acp-2019-1117

Zhu, L., Jacob, D. J., Keutsch, F. N., Mickley, L. J., Scheffe, R., Strum, M., et al. (2017). Formaldehyde (HCHO) as a hazardous air pollutant: Mapping surface air concentrations from satellite and inferring cancer risks in the United States. *Environmental Science & Technology*, *51*(10), 5650–5657. https://doi.org/10.1021/acs.est.7b01356

Zhu, L., Jacob, D. J., Kim, P. S., Fisher, J. A., Yu, K., Travis, K. R., et al. (2016). Observing atmospheric formaldehyde (HCHO) from space: Validation and intercomparison of six retrievals from four satellites (OMI, GOME2A, GOME2B, OMPS) with $SEAC^4RS$ aircraft observations over the southeast US. *Atmospheric Chemistry and Physics*, *16*(21), 13477–13490. https://doi.org/10.5194/acp-16-13477-2016

Zhu, L., Jacob, D. J., Mickley, L. J., Marais, E. A., Cohan, D. S., Yoshida, Y., et al. (2014). Anthropogenic emissions of highly reactive volatile organic compounds in eastern Texas inferred from oversampling of satellite (OMI) measurements of HCHO columns. *Environmental Research Letters*, *9*(11), 114004. https://doi.org/10.1088/1748-9326/9/11/114004

Zhu, L., Mickley, L. J., Jacob, D. J., Marais, E. A., Sheng, J., Hu, L., et al. (2017). Long-term (2005–2014) trends in formaldehyde (HCHO) columns across North America as seen by the OMI satellite instrument: Evidence of changing emissions of volatile organic compounds. *Geophysical Research Letters*, *44*, 7079–7086. https://doi.org/10.1002/2017GL073859

Zhu, S., Li, X., Yu, C., Wang, H., Wang, Y., & Miao, J. (2018). Spatiotemporal variations in satellite-based formaldehyde (HCHO) in the Beijing–Tianjin–Hebei region in China from 2005 to 2015. *Atmosphere*, *9*(1), 5. https://doi.org/10.3390/atmos9010005